ELSEVIER

Chemistry & Biology 8 (2001) 611–625

Chemistry & Biology

www.elsevier.com/locate/chembiol

Research Paper

Helical peptide models for protein glycation: proximity effects in catalysis of the Amadori rearrangement

Janani Venkatraman [a], Kamna Aggarwal [a], P. Balaram [a,b,*]

[a] *Molecular Biophysics Unit, Indian Institute of Science, Bangalore 560012, India*

[b] *Chemical Biology Unit, Jawaharlal Nehru Centre for Advanced Scientific Research, Jakkur Campus, Jakkur P.O., Bangalore 560004, India*

Received 24 November 2000; revisions requested 6 February 2001; revisions received 1 March 2001; accepted 20 April 2001
First published online 8 May 2001

Abstract

Introduction: Non-enzymatic glycation of proteins has been implicated in various diabetic complications and age-related disorders. Proteins undergo glycation at the N-terminus or at the ε-amino group of lysine residues. The observation that only a fraction of all lysine residues undergo glycation indicates the role of the immediate chemical environment in the glycation reaction. Here we have constructed helical peptide models, which juxtapose lysine with potentially catalytic residues in order to probe their roles in the individual steps of the glycation reaction.

Results: The peptides investigated in this study are constrained to adopt helical conformations allowing residues in the *i* and *i*+4 positions to come into spatial proximity, while residues *i* and *i*+2 are far apart. The placing of aspartic acid and histidine residues at interacting positions with lysine modulates the steps involved in early peptide glycation (reversible Schiff base formation and its subsequent irreversible conversion to a ketoamine product, the Amadori rearrangement). Proximal positioning of aspartic acid or histidine with respect to the reactive lysine residue retards initial Schiff base formation. On the contrary, aspartic acid promotes catalysis of the Amadori rearrangement. Presence of the strongly basic residue arginine proximate to lysine favorably affects the pK_a of both the lysine ε-amino group and the singly glycated lysine, aiding in the formation of doubly glycated species. The Amadori product also formed carboxymethyl lysine, an advanced glycation endproduct (AGE), in a time-dependent manner.

Conclusions: Stereochemically defined peptide scaffolds are convenient tools for studying near neighbor effects on the reactivity of functional amino acid sidechains. The present study utilizes stereochemically defined peptide helices to effectively demonstrate that aspartic acid is an efficient catalytic residue in the Amadori arrangement. The results emphasize the structural determinants of Schiff base and Amadori product formation in the final accumulation of glycated peptides.

Keywords: Amadori rearrangement; Catalysis; Electrospray ionization mass spectrometry; Protein glycation; Helical peptide model

1. Introduction

Non-enzymatic glycation of proteins has been implicated as an important cause of the complications associated with diabetes [1–4]. The Maillard hypothesis suggests that chemical modification of proteins by glucose and subsequent reactions of the adduct may result in products which are directly responsible for many pathological conditions in diabetes [1,5,6]. The reaction of glucose with amino groups in proteins results in the reversible formation of a Schiff base or aldimine, which can undergo irreversible Amadori rearrangement (Fig. 1) to form a ketoamine product. Glycation is also a process that appears to be associated with age-related disorders and may be particularly important in the context of long-lived proteins which do not undergo rapid synthesis and turnover [3,7–14].

The initial observation that hemoglobin was glycated in vivo [15,16], specifically at the N-terminus of the β-chain (Val1β), triggered off a very large number of investigations on the non-enzymatic glycation of proteins in vivo and in vitro. The purpose of many such studies was the characterization of site-specificity of glycation and the factors catalyzing rearrangement to the Amadori product. While hemoglobin has inevitably been the focus of the majority of mechanistic investigations [17–21], the glycation of a

* Correspondence: P. Balaram;
E-mail: pb@mbu.iisc.ernet.in

1074-5521/01/$ – see front matter
PII: S1074-5521(01)00036-9

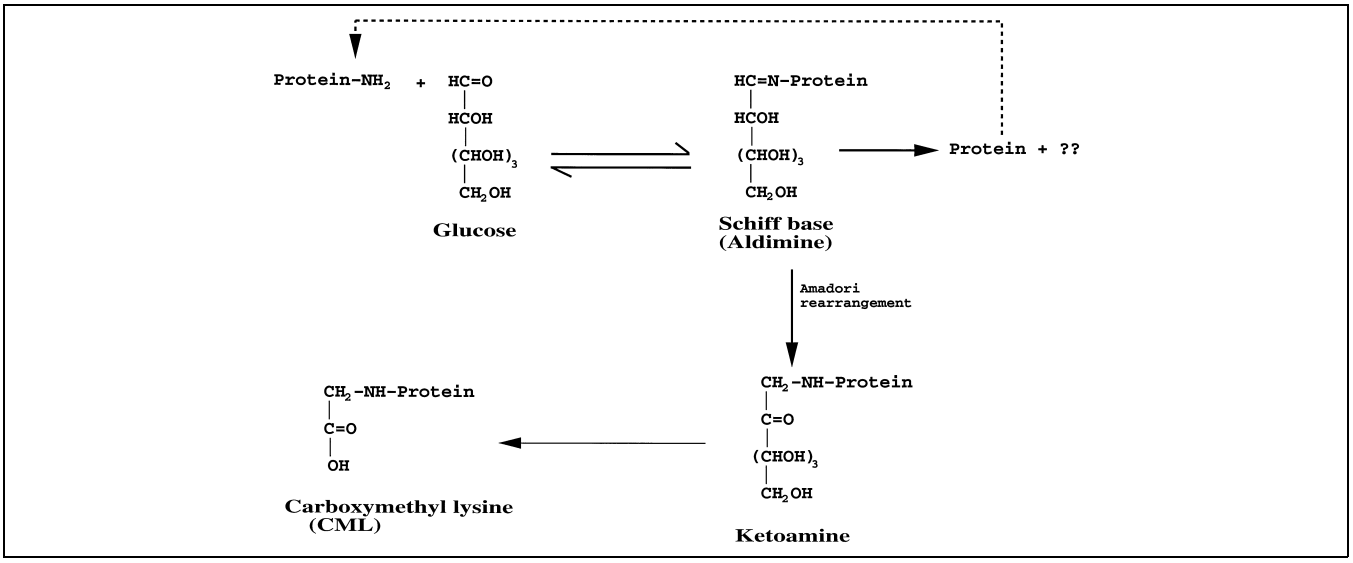

Fig. 1. Schematic representation of the reactions involved in the glycation of proteins. The open chain form of the sugar (glucose) reacts with the ε-amino group of lysine residues to form a Schiff base, which undergoes the Amadori rearrangement to form a ketoamine product. This ketoamine is subject to a series of reactions which result in AGEs, one of which is CML.

variety of other proteins, notably albumin [22,23], α- and β-crystallins [24], collagen [25], RNase A [26,27], human and horse liver alcohol dehydrogenase [28], Cu–Zn-superoxide dismutase [29] and various erythrocytic proteins [29–32], has also been studied.

Non-enzymatic glycation of proteins involves modification of, primarily, the ε-amino group of lysine and the free N-terminus. But, only a small proportion of all lysyl residues undergoes glycation. It has been suggested that the immediate chemical environment of an amino group modulates the glycation reaction. Factors affecting the pK_a of the amino group would be instrumental in determining the rate of formation of Schiff base adducts, while the proximity of groups capable of proton abstraction augments the efficiency of the rearrangement reaction, to form the ketoamine product. Proposed sites of preferential Schiff base formation are stretches of lysyl residues [19] (e.g.

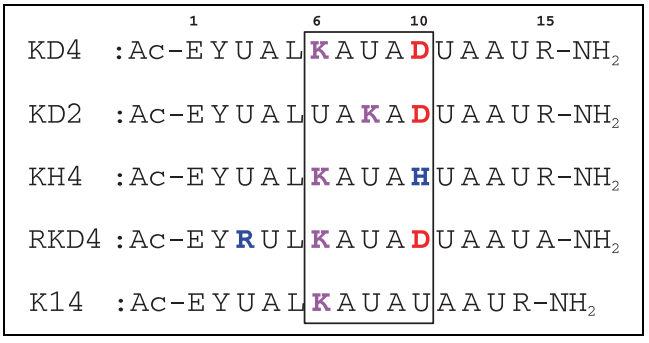

Fig. 2. Sequences of synthetic peptides used as glycation models. The potential glycation site (Lys6) is in purple, while acidic (Asp10) and basic residues (His10/Arg3) are in red and blue, respectively.

The principle glycation site of albumin, Lys525, lies in a Lys–Lys sequence [22,23]) and the N-terminus of proteins characterized by its low pK_a (e.g. N^{α}-Lys1 in RNase A [26]). Factors suggested to influence the Amadori rearrangement are imidazole groups of histidine residues [23,28], carboxylate groups of acidic residues [19,26] and bound phosphate ions and other negatively charged ions [26,33]. The role of some proposed amino acid catalysts has been studied in model di- and tri-peptides and the presence of histidine was shown to accelerate the glycation reaction [34,35].

The purpose of the present study is to examine the role of spatially proximate residues on the formation of the aldimine and its subsequent rearrangement to the Amadori product. Towards this end, we have designed a series of helical peptides containing a single, centrally positioned lysyl residue to serve as a glycation site. In two of the sequences listed in Fig. 2, we have chosen to vary the relative positioning of a potential catalytic residue for the Amadori reaction, aspartic acid (KD4/KD2). In peptide KH4, the aspartyl residue of peptide KD4 has been replaced by the basic histidine residue, while peptide RKD4 has both acidic (aspartic acid) and basic (arginine) residues flanking the lysine. The choice of sequences was based on the fact that in peptide helices, residues *i* and *i*+4 lie on the same face of the helix, while residues *i* and *i*+2 are spatially far apart (Fig. 3). Helical conformations in the designed peptides were nucleated and stabilized by introduction of the α,α-dialkyl residue (α-aminoisobutyric acid, Aib, U) at four positions. The ability of Aib residues to stabilize helical conformations in oligopeptides has been extensively demonstrated by crystallographic studies [36–40]. Spectroscopic studies in solution establish that pep-

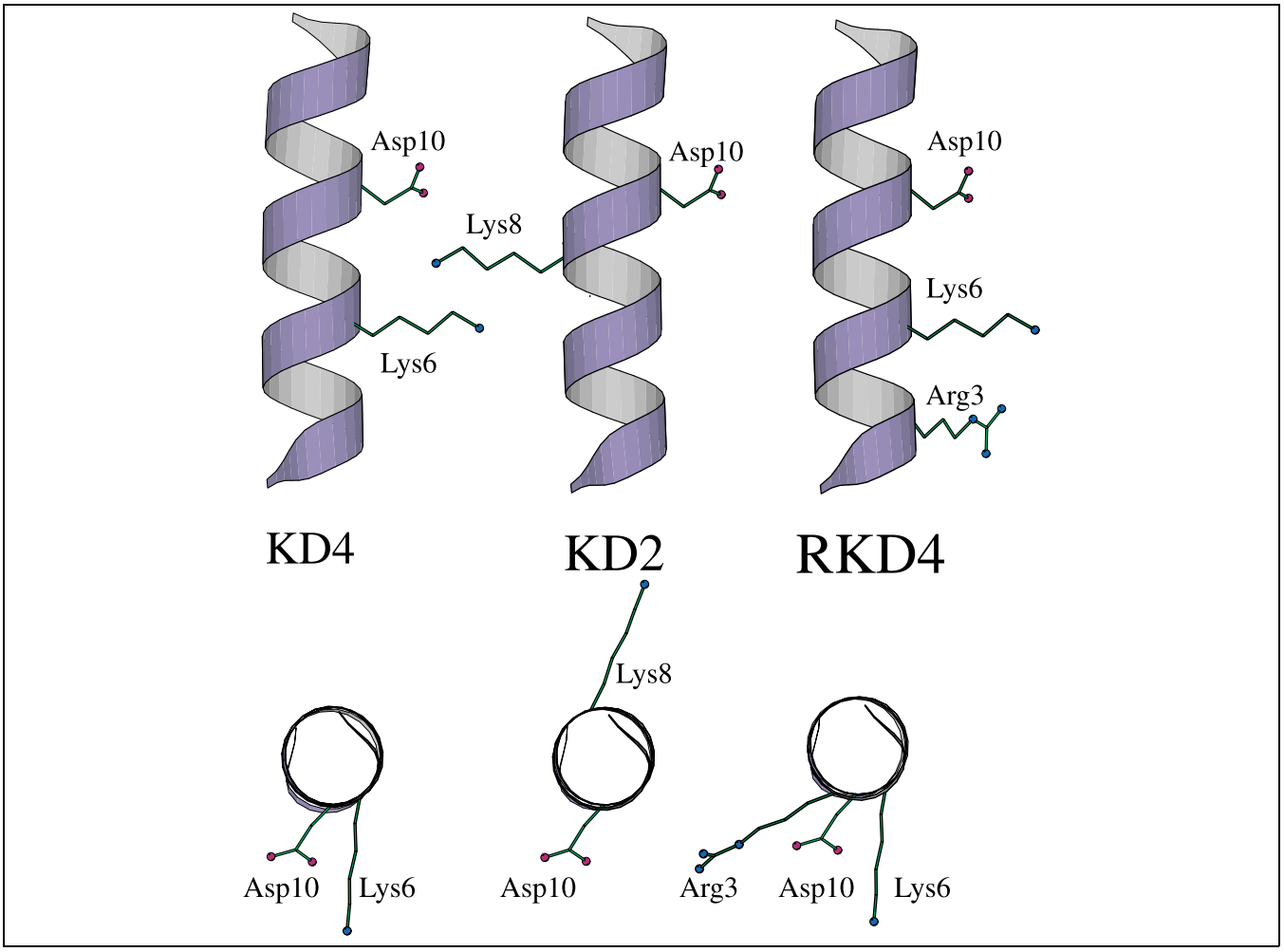

Fig. 3. Spatial juxtaposition of Lys6 (the glycation site) and the catalytic aspartic acid in a peptide helix, viewed perpendicular to (top panel) and down (bottom panel) the helix axis. Lys6 and Asp10 are proximate in KD4, while Lys6 and Asp8 are far apart in KD2. In RKD4, Arg3 and Asp10 lie on the same helix face as Lys6.

tides of length less than 20 residues which contain three or four Aib residues, adopt largely helical conformations [41,42]. In the present study, the incorporation of four Aib residues in a 15 residue sequence is anticipated to result in the formation of a relatively well-defined helical scaffold upon which the functional side chains are arrayed. The peptide termini were chemically blocked with an acetyl group at the N-terminus and a carboxamide moiety at the C-terminus. This allows for an additional hydrogen bond to be formed at each end of the helix, reducing the number of unsatisfied NH and CO groups [43]. A peptide, K14, which contained only the reactive site lysine with no prospective catalytic residues in close proximity, served as a control for evaluating neighboring group effects. This peptide was accidentally obtained as a deletion product during the synthesis of peptide KH4 (His10 deleted). The results described in this paper establish that the proximal carboxylate of Asp serves as the internal catalyst of the Amadori rearrangement in the designed peptides KD4 and RKD4.

2. Results

2.1. Circular dichroism of peptides

The far UV CD spectra of all five peptides (Fig. 4) in methanol resemble classical helical patterns with negative bands at 208 nm and between 220 and 222 nm [44,45]. Values of molar ellipticity at 222 nm, which is considered an index of helix content, either exceeded (peptide KH4) or were comparable (peptides RKD4 and KD2) to those observed for model alanine-based peptides studied by Baldwin and co-workers [46]. The presence of a tyrosine residue (which contributes to the CD signal at 222 nm [47]) precludes accurate estimation of helix content. Furthermore, in constrained peptides where helicity has been induced by introduction of folding nuclei, observed ellipticities greatly exceed that anticipated for '100% helix' based on earlier models [48]. However, the amino acid composition of all five peptides is very similar, as is the length, and hence relative helicities can be compared.

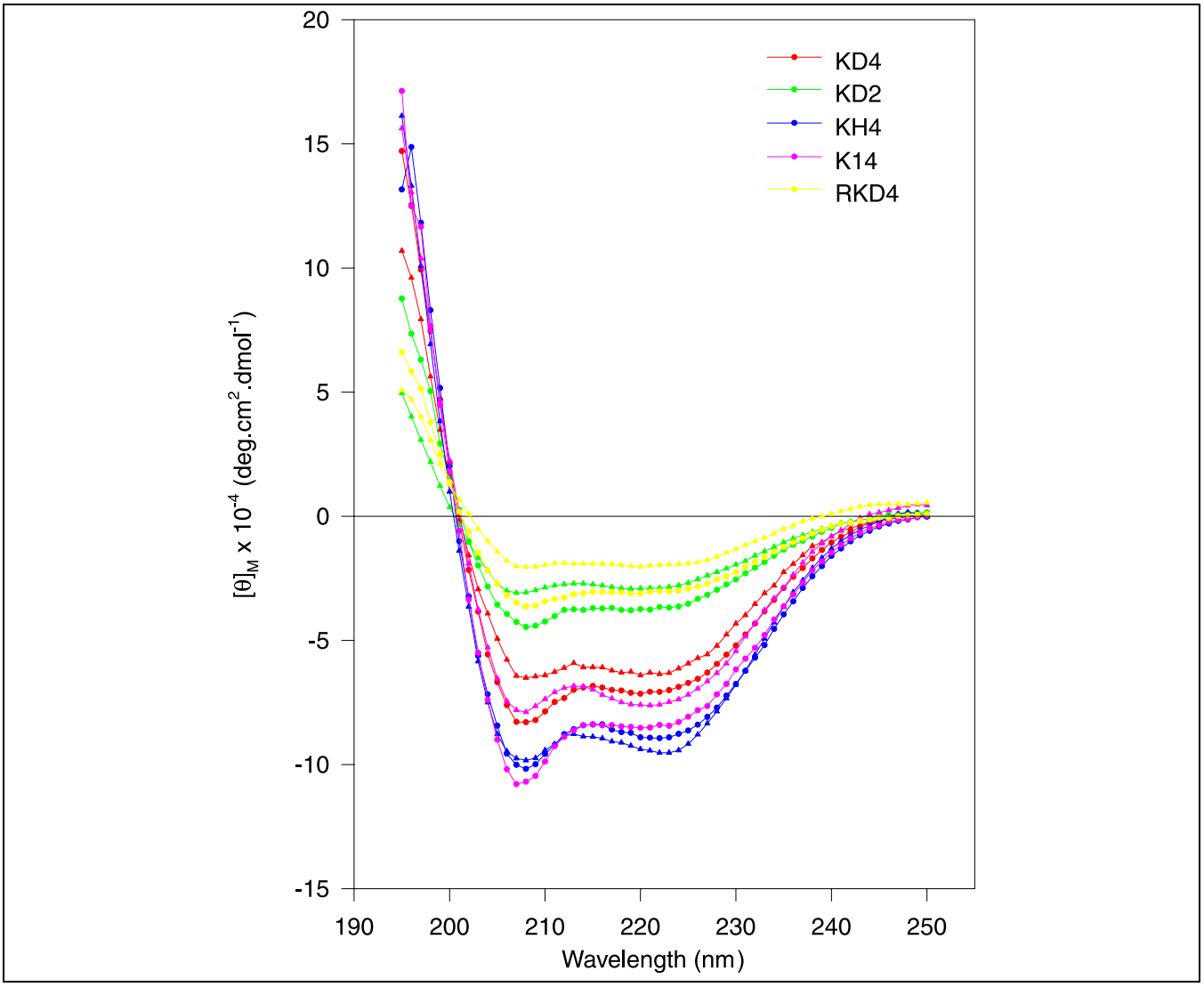

Fig. 4. CD spectra of peptides KD4 (red), KD2 (green), KH4 (blue), K14 (pink) and RKD (yellow) in 100% methanol (○) and 50% water/methanol mixtures (△).

Peptide K14 is shorter by a residue, but this is not expected to have a significant influence on the intrinsic helicity.

The extent of helicity follows the order KH4 > K14 > KD4 > KD2 > RKD4. In all cases, there is a small reduction in helicity in 50% methanol/water mixtures, which is expected in view of the tendency of water to compete for backbone hydrogen-bonding sites. Peptide KH4 and KD4, characterized by the most intense CD bands, are the most structured, perhaps due to structure-stabilizing interactions between residues Lys6 and Asp10 (in KD4) or the deprotonated form of His10 (in KH4), while the CD spectrum of the dibasic RKD4 suggests that it is least helical. In all cases, the CD data suggest that a substantial fraction of peptide molecules in solution adopt folded helical structures, permitting further discussion of reactions to be based on the assumption of a helical scaffold.

2.2. *Mass spectrometry (MS) of peptides and glycated peptides*

MS is a convenient technique for monitoring reactions involving changes in reactant masses. Both matrix-assisted laser desorption ionization (MALDI) and electrospray ionization (ESI)-MS have been utilized for the qualitative as well as quantitative measurement of glycated proteins and peptides [49,50] and the characterization of the advanced glycation products in the Maillard reaction [51–59]. ESI-MS has therefore been utilized in this investigation to monitor the rate of glycation of the designed peptides and to identify the various reaction intermediates.

The progress of the glycation reaction can be detected using MS as an increase in mass over that of the peptide under investigation. The change in mass corresponds to the addition of a glucose moiety with the concomitant loss of a water molecule ($\Delta M_r = 162$). All five peptides

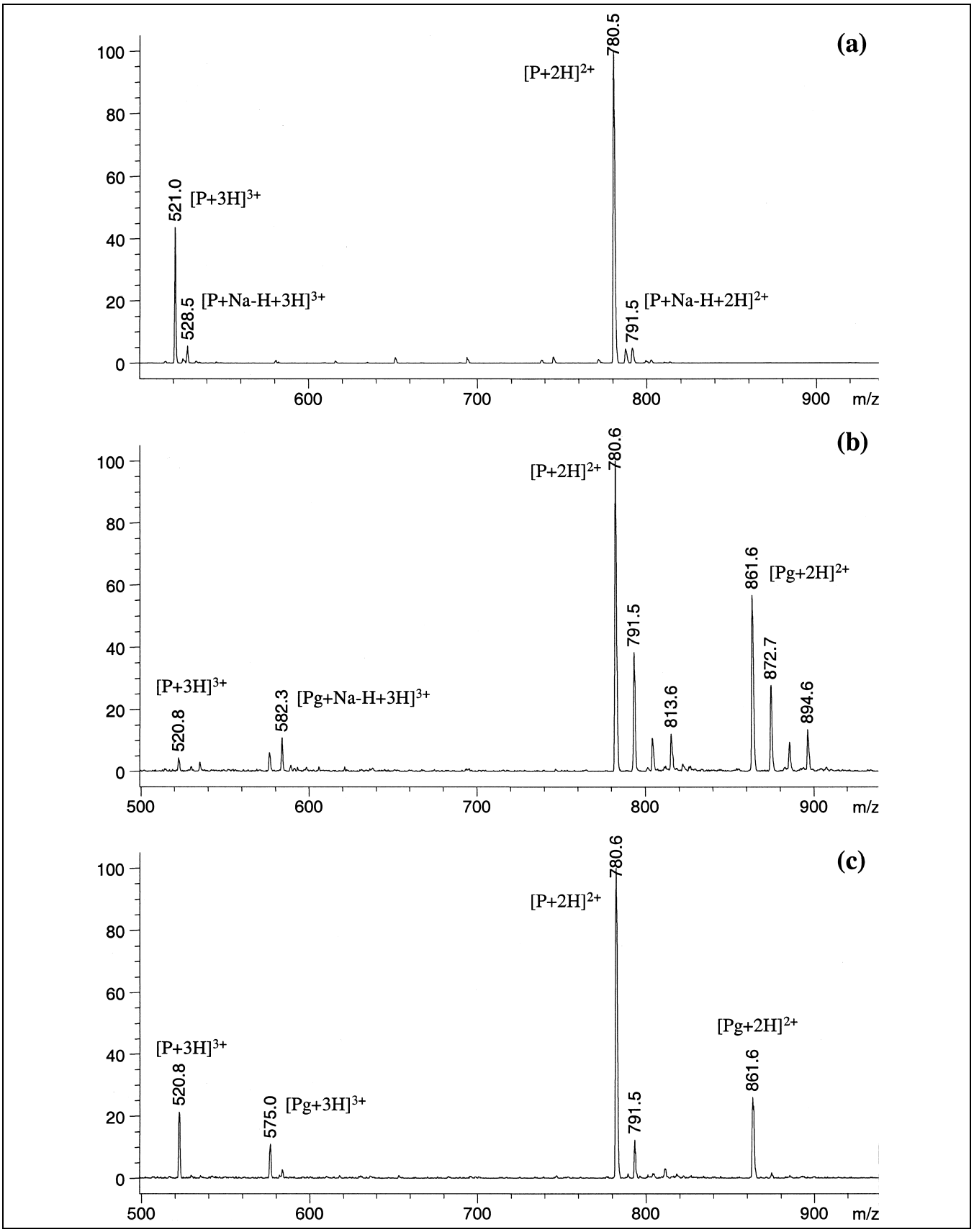

Fig. 5. ESI mass spectra of peptide KD4 (a) showing various charge states observed, (b) 44 h into the glycation reaction (the spectrum shows charge states corresponding to both peptide (e.g. $[P+2H]^{2+}$) and glycated peptide (e.g. $[Pg+2H]^{2+}$), see Table 1 for full listing of all charge states observed) and (c) 44 h into the glycation reaction after treatment with hydroxylamine. This glycated species corresponds to the fraction of all glycated KD4 that has undergone the Amadori rearrangement and is hence the ketoamine product.

used in the present investigation (KD4/KD2/KH4/RKD4/K14) have two or three basic residues and hence the capacity to pick up multiple protons to form higher charged species. The peptide KD4 has the potential to acquire two protons, one each on the basic lysine and arginine residues. The observation of triply charged ions in KD4 (Fig. 5a) is rationalized by the ability of peptide helices to be protonated at the C-terminus, where between two and three free backbone carbonyl groups are available. Notably, in a helical conformation, the negatively charged end of the helix macrodipole is placed at the C-terminus, facilitating protonation and metallation even in neutral, apolar helical peptides, under electrospray conditions (unpublished results). In addition, the carboxyl groups of the residues aspartic acid and glutamic acid can form sodium adducts. The MS analysis of such a heterogeneous mixture reveals multiple peaks corresponding to the various proton/sodium adducts with appropriate *m*/*z* values. Fig. 5a, the mass spectrum of peptide KD4, shows the presence of a doubly protonated species ($[P+2H]^{2+}$, *m*/*z* 780.5), a doubly charged sodium adduct ($[P+Na-H+2H]^{2+}$, *m*/*z* 791.5), a triply protonated species ($[P+3H]^{3+}$, *m*/*z* 521.0) and a triply charged sodium adduct ($[P+Na-H+3H]^{3+}$, *m*/*z* 528.5). Fig. 5b, the mass spectrum of KD4 recorded 44 h into the glycation reaction, shows many such multiply charged adducts for both the intact peptide as well as its glycated form. Table 1 lists the charged species observed for the free and glycated forms of all five peptides.

2.3. Glycation of peptides KD4, KD2, KH4 and K14

Peptide glycation was investigated under different conditions of pH (pH 6.5, 7.5 and 8.5) and temperature (room temperature and 37°C) for peptides KD4 and KD2. No glycation was observed at pH 6.5 for both peptides. At room temperature, glycation was faster at pH 8.5 than at pH 7.5. On the contrary, at 37°C, glycation rates were comparable for both conditions of pH. This similarity in the glycation rates at pH 7.5 and 8.5 at 37°C was observed for peptides K14 and KH4 as well. Hence, all data considered for discussion in this report were acquired at pH 8.5 and 37°C.

The lysine residue of each peptide formed adducts with glucose under the experimental conditions studied. Figs. 5b, 6a, 7a and 8a are representative spectra for the glycation of KD4, KD2, KH4 and RKD4, respectively. The glycated species observed in these spectra include both aldimine and ketoamine forms, which are isomeric and hence indistinguishable by ESI and MS under conditions where only multiply charged molecular ions are detected. Fig. 9 depicts the glycation reaction of KD4, KD2, KH4 and K14 as a function of time (The differences in the time scales for the two groups of peptides, KD4/KD2 and KH4/K14, are because of widely different rates of glycation and subsequent reactions). The relative intensities of the peaks corresponding to glycated and intact peptides in the mass spectra were used as an index of the glycation reaction. Complex reaction profiles are observed in all

Table 1
Charge states observed for peptides KD4, KD2, KH4 and RKD4 and their various glycated forms

Peptide	Charged species observed	*m*/*z* (Da)		
		Peptide (P)	Peptide+glucose (Pg)	Peptide+2glucose
KD4	$[M+2H]^{2+}$	780.5	861.6	
M_{calc} = 1559.6 Da	$[M+Na-H+2H]^{2+}$	791.5	872.7	
	$[M+2Na-2H+2H]^{2+}$	802.5	883.7	
	$[M+3Na-3H+2H]^{2+}$	813.6	894.6	
	$[M+3H]^{3+}$	520.8	575.0	
	$[M+Na-H+3H]^{3+}$	528.3	582.3	
KD2	$[M+2H]^{2+}$	780.6	861.8	
M_{calc} = 1559.6 Da	$[M+Na-H+2H]^{2+}$	791.7	872.8	
	$[M+2Na-2H+2H]^{2+}$	802.6	883.7	
	$[M+3Na-3H+2H]^{2+}$	813.6	894.6	
	$[M+3H]^{3+}$	520.8	574.8	
	$[M+Na-H+3H]^{3+}$	528.2	582.0	
KH4	$[M+2H]^{2+}$	791.5	872.7	
M_{calc} = 1581.6 Da	$[M+Na-H+2H]^{2+}$	802.5	883.6	
	$[M+2Na-2H+2H]^{2+}$	813.5	894.5	
	$[M+3H]^{3+}$	528.4	582.2	
KH4-CML M_{calc} = 1639.6 Da	$[M+2H]^{2+}$		820.5	
RKD2	$[M+2H]^{2+}$	780.5	861.5	943.3
M_{calc} = 1559.6 Da	$[M+Na-H+2H]^{2+}$	791.5	872.5	954.3
	$[M+2Na-2H+2H]^{2+}$	802.5	883.5	
	$[M+3Na-3H+2H]^{2+}$	813.5	894.5	
	$[M+3H]^{3+}$	520.8	574.8	628.9
	$[M+Na-H+3H]^{3+}$	528.0	582.2	636.2
	$[M+2Na-2H+3H]^{3+}$	535.3	589.5	

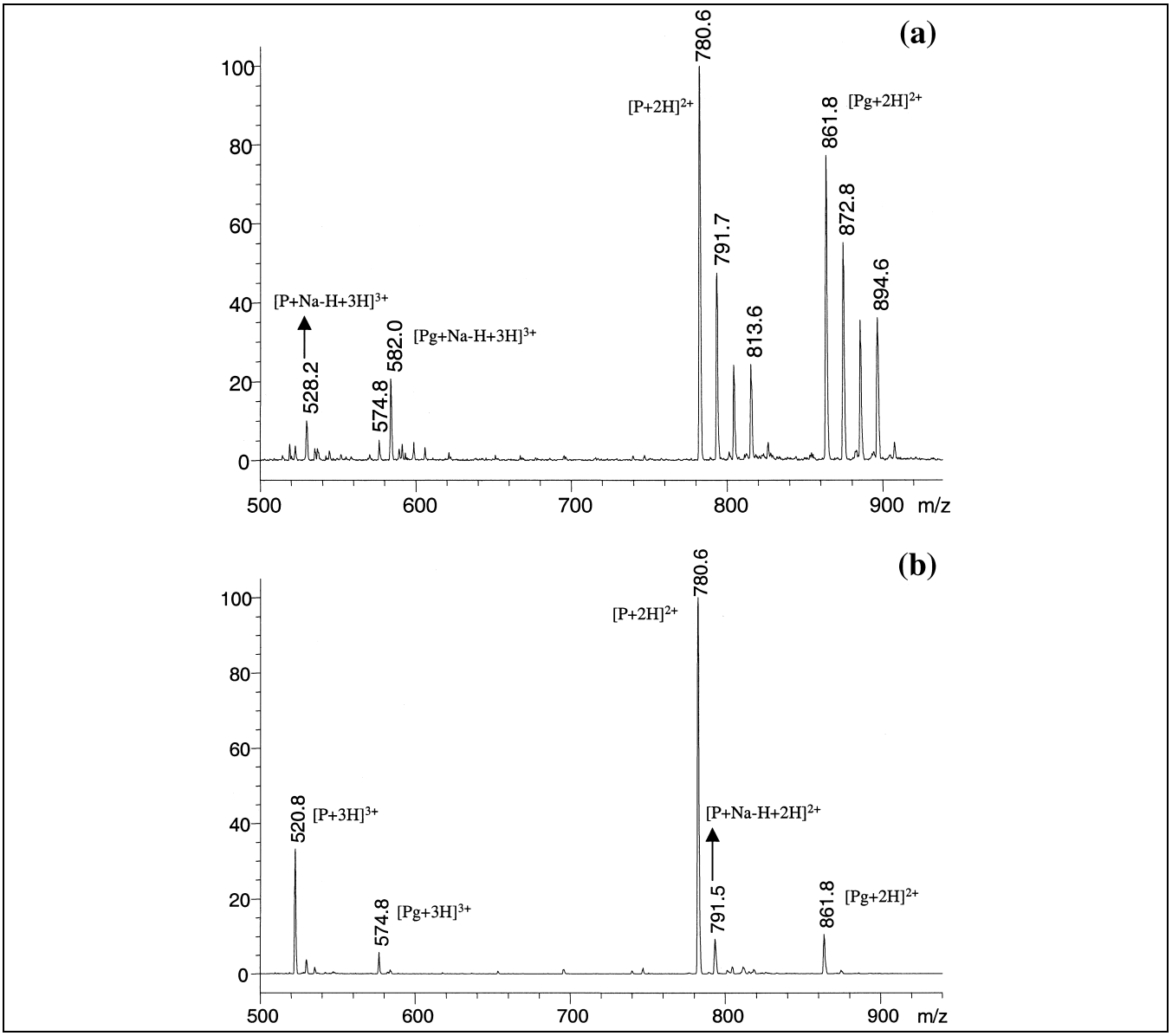

Fig. 6. ESI mass spectra of peptide KD2 (a) 44 h into the glycation reaction (the spectrum shows charge states corresponding to both peptide (e.g. $[P+2H]^{2+}$) and glycated peptide (e.g. $[Pg+2H]^{2+}$)) and (b) 44 h into the glycation reaction after treatment with hydroxylamine. Here too, the peaks in the mass spectrum correspond to the ketoamine product. Comparison of (b) with Fig. 5c reveals less ketoamine formation in the case of KD2 than KD4.

four peptides. In all four cases, the glycation reaction appears to pass through distinct stages. Initial appearance of the glucose adduct is very rapid with near linear reaction kinetics. The reaction then briefly saturates, followed by a decrease in total glycation. Amounts of glycated peptide then increase again and soon saturate. While the reaction profile of glycation is similar for the four peptides, efficiency of glycation varies in terms of maximum glycation observed, time taken for the reaction to reach saturation and the magnitude of the decrease interrupting saturation. Maximum glycation is observed in K14 (with 76% of total peptide being glycated at 3 h), followed by KH4 (62% at 6 h) and KD2 (60% at 23 h), while KD4 showed least total glycation (44% at saturation). Peptide KD4 was also the first to attain saturation and showed the least decrease in glycation amounts. This dip was most prominent in K14, with the subsequent rise also being low.

2.4. Amadori product formation in peptides KD4, KD2, KH4 and K14

In order to probe the rates of Amadori product formation, it is important to accurately differentiate between the aldimine and ketoamine forms of the glycated peptides. The lability of the aldimine linkage, and consequent reversal of Schiff base formation, has been well documented. Studies on the formation of Schiff base adducts between hemoglobin and aliphatic and aromatic aldehydes [60] re-

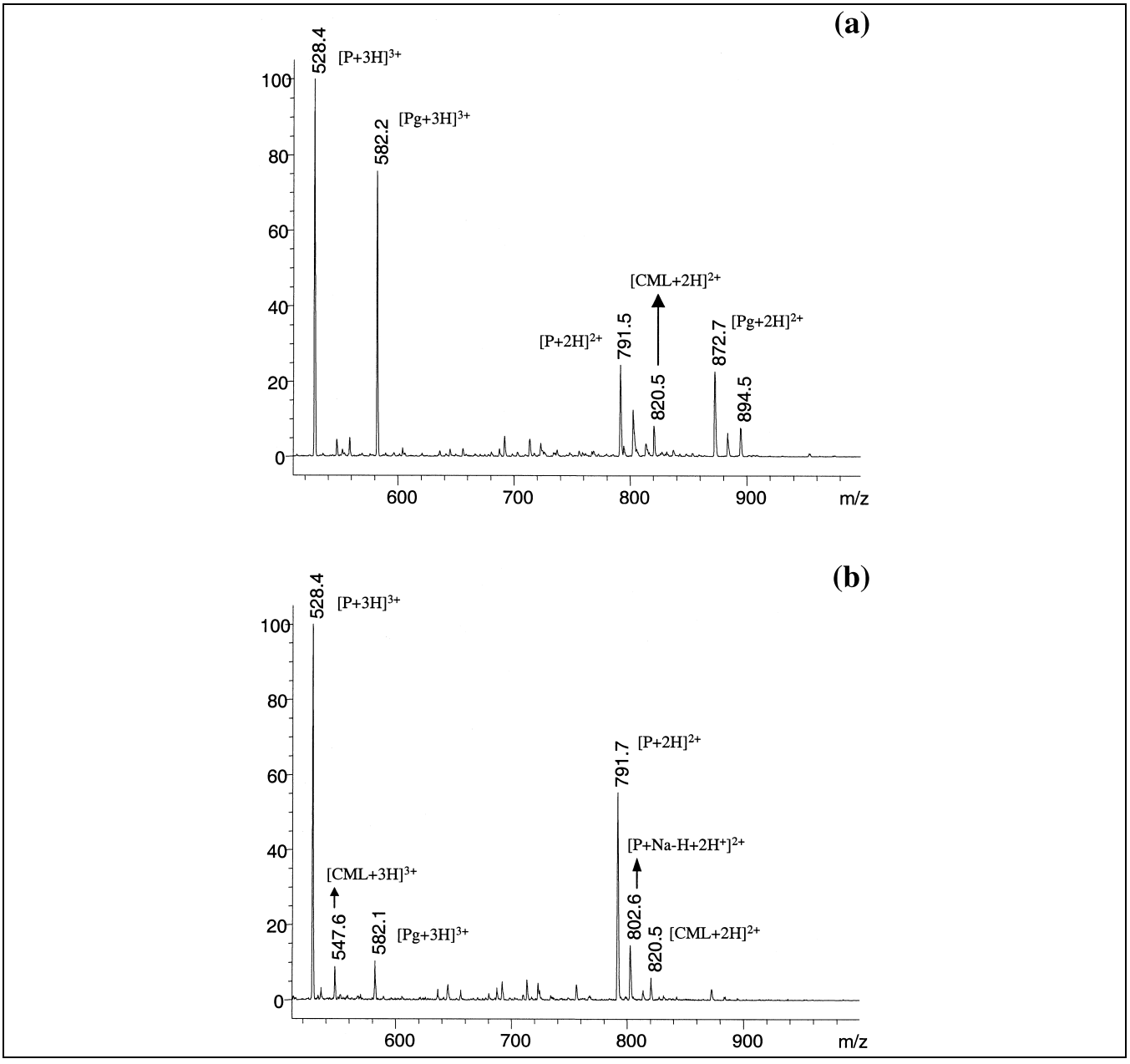

Fig. 7. ESI mass spectra of peptide KH4 (a) 48 h into the glycation reaction, showing charge states corresponding to both peptide (e.g. $[P+2H]^{2+}$) and glycated peptide (e.g. $[Pg+2H]^{2+}$) and (b) 48 h into the glycation reaction after treatment with hydroxylamine, showing peaks corresponding to the ketoamine product. Comparison of (b) with Fig. 5c reveals less ketoamine formation in KH4 than KD4. Also seen in both spectra is a peak at *m*/*z* 820.5 which corresponds to the doubly charged carboxymethylated derivative of the peptide (CML).

veal that such linkages are susceptible to dialysis against aldehyde free buffers. Isbell and Frush [61] showed that glycosylamines are hydrolyzed in weakly acidic solutions, with maximum hydrolysis observed near pH 5.0. In addition, *trans* Schiff base reactions are observed on treatment with hydrazine derivatives such as phenylhydrazine [62,63], with release of the free amine. This reaction is used in the displacement of pyridoxal phosphate from

→

Fig. 8. ESI mass spectra of peptide RKD4 (a) 24 h into the glycation reaction, (b) 24 h into the glycation reaction after treatment with hydroxylamine and (c) 126 h into the glycation reaction. Comparison of (b) with Fig. 5c reveals equivalent amounts of ketoamine formation in peptide RKD4 as compared to KD4. (c) Shows peaks corresponding to the doubly glycated form of peptide RKD4. Also seen in (b) and (c) are peaks at *m*/*z* 515.5 and 569.5 which correspond to dehydrated RKD4 and glycated RKD4, respectively. The amidated C-terminus of peptide RKD4 could have undergone dehydration to yield the nitrile. The greater ability of the nitrile to get protonated as compared to the amidated C-terminus of the peptide could be reflected in the observation that only the triply charged species is observed in mass spectra.

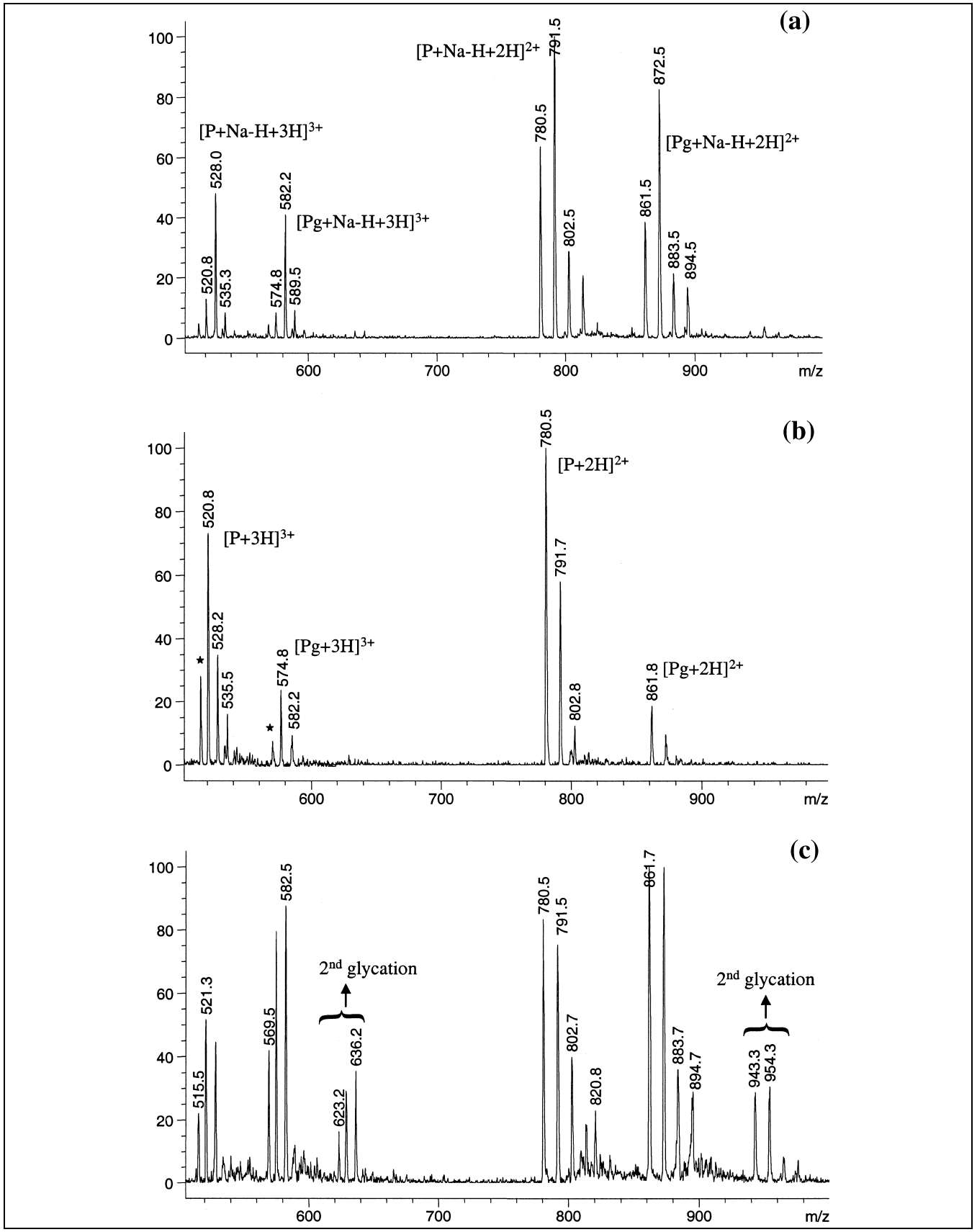
(a)
[P+Na-H+2H]2+
791.5
872.5
780.5
[P+Na-H+3H]3+
[Pg+Na-H+2H]2+
528.0
582.2
[Pg+Na-H+3H]3+
861.5
802.5
883.5
894.5
520.8
535.3
574.8
589.5
100
80
60
40
20
0
600
700
800
900
m/z
(b)
780.5
[P+2H]2+
520.8
[P+3H]3+
791.7
528.2
[Pg+3H]3+
574.8
535.5
582.2
861.8
[Pg+2H]2+
802.8
(c)
582.5
861.7
780.5
791.5
2nd glycation
521.3
569.5
802.7
883.7
894.7
636.2
820.8
943.3
954.3
515.5
623.2

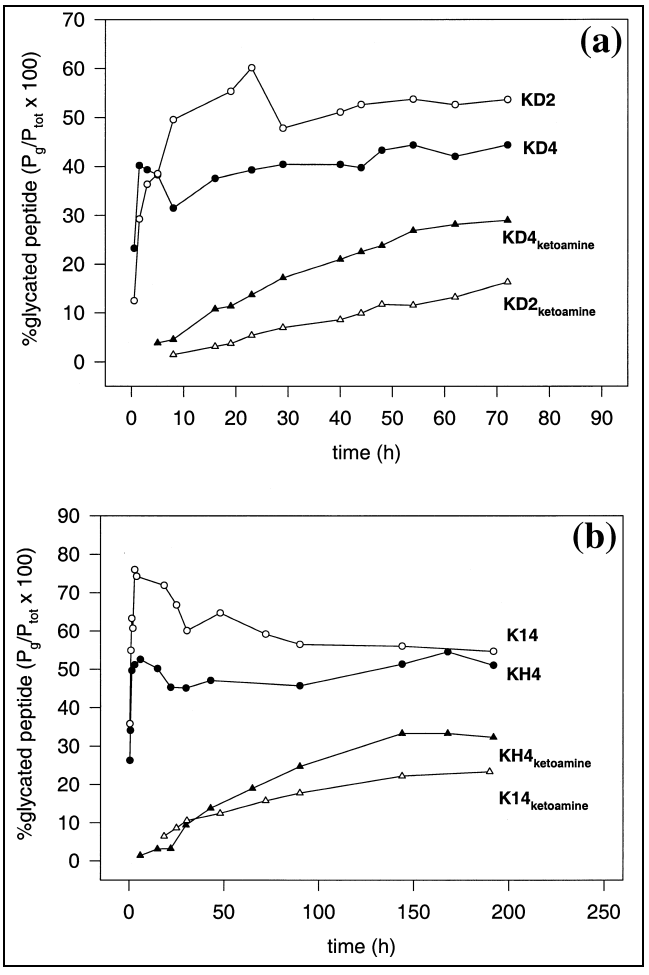

Fig. 9. Time course of the glycation reaction for peptides KD4, KD2, KH4 and K14. (a) Compares the rate of total glycation and ketoamine formation in peptides KD4 (●, ▲) and KD2 (○, △). Glycated peptide amounts are represented as a percentage of total peptide amounts in the reaction mixture (glycated+unglycated peptide). (b) Performs the same comparison for peptides KH4 (●, ▲) and K14 (○, △).

proteins bearing the coenzyme as a Schiff base [64]. Acharya and Manning [65] have also used phenylhydrazine to distinguish between aldimine and ketoamine forms of the glyceraldehyde adducts of hemoglobin A. The relative lability of the aldimine linkage in the presence of nucleophilic, hydrazine derivatives has been utilized to differentiate between the Schiff base and the Amadori product. The reagent hydroxylamine, which rapidly causes release of free amino groups from glucose–amine Schiff base adducts, has been used for this purpose in our studies.

Incubating the glycated peptide with hydroxylamine for 15 min caused complete conversion of the Schiff base adduct to the unglycated peptide. MS analysis of the resultant sample revealed estimates of Amadori product formation since the ketoamine is unreactive under these conditions. It may be noted that, in principle, oxime formation may be anticipated; but model experiments demonstrated that this occurs only under forcing conditions. The Amadori rearrangement product formed earliest in the case of KD4 (Fig. 9a) with appearance of Amadori product as early as 5 h. In addition, approximately twice as much Amadori product was observed for KD4 (~30% of total peptide amounts, or 66% of glycated peptide amounts) as KD2 after 3 days. KH4 demonstrated a greater potential to catalyze the Amadori reaction than KD2, with Amadori product amounts equalling that of KD4 when saturation was reached. However, the catalytic efficiency was lower, with KH4 requiring 7 days to produce ketoamine levels comparable to that of KD4. The control peptide K14 demonstrated poor conversion potential with only 23% of total peptide bearing the Amadori product even after 8 days.

2.5. The glycation reaction in peptide RKD4

While it was observed that aspartic acid catalyzed the Amadori rearrangement reaction, rate of Schiff base formation was poor in KD4 and appeared to be best under conditions where no catalytic residue was present (peptide K14). It could be argued that a strongly basic residue proximate to the lysine residue might ameliorate the effect of aspartic acid and favorably affect the pK_a of Lys6, resulting in rapid accumulation of aldimine adducts. RKD4 would combine both features and have the basic arginine residue and the catalytic aspartic acid residue flanking the reactive site lysine. The initial glycation reaction paralleled that of KH4 (45% of total peptide was glycated at 9 h) and initial ketoamine formation was sim-

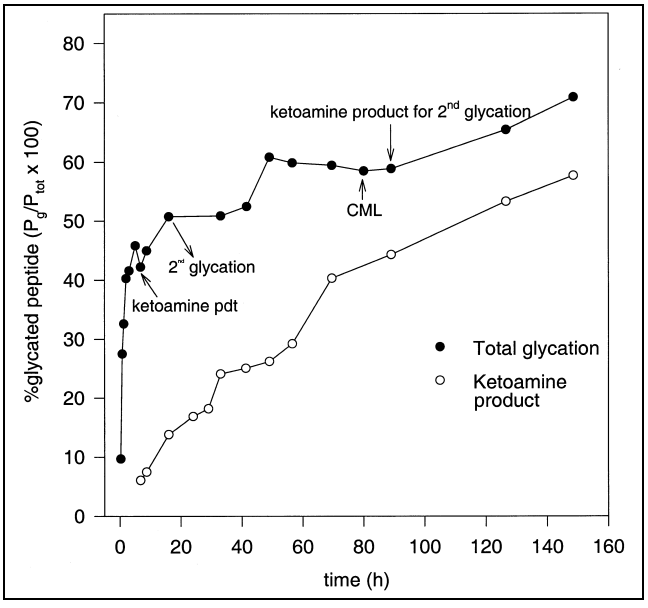

Fig. 10. Time course of the glycation reaction for peptide RKD4. Total glycation (●) is compared with formation of ketoamine and other products resistant to hydrolysis by hydroxylamine (○). Also indicated are the approximate times of appearance of readily detectable amounts of the ketoamine product, the bis-glucose adduct of lysine, the carboxy methylated derivative of mono-glycated lysine and the ketoamine product of the bis-glucose adduct.

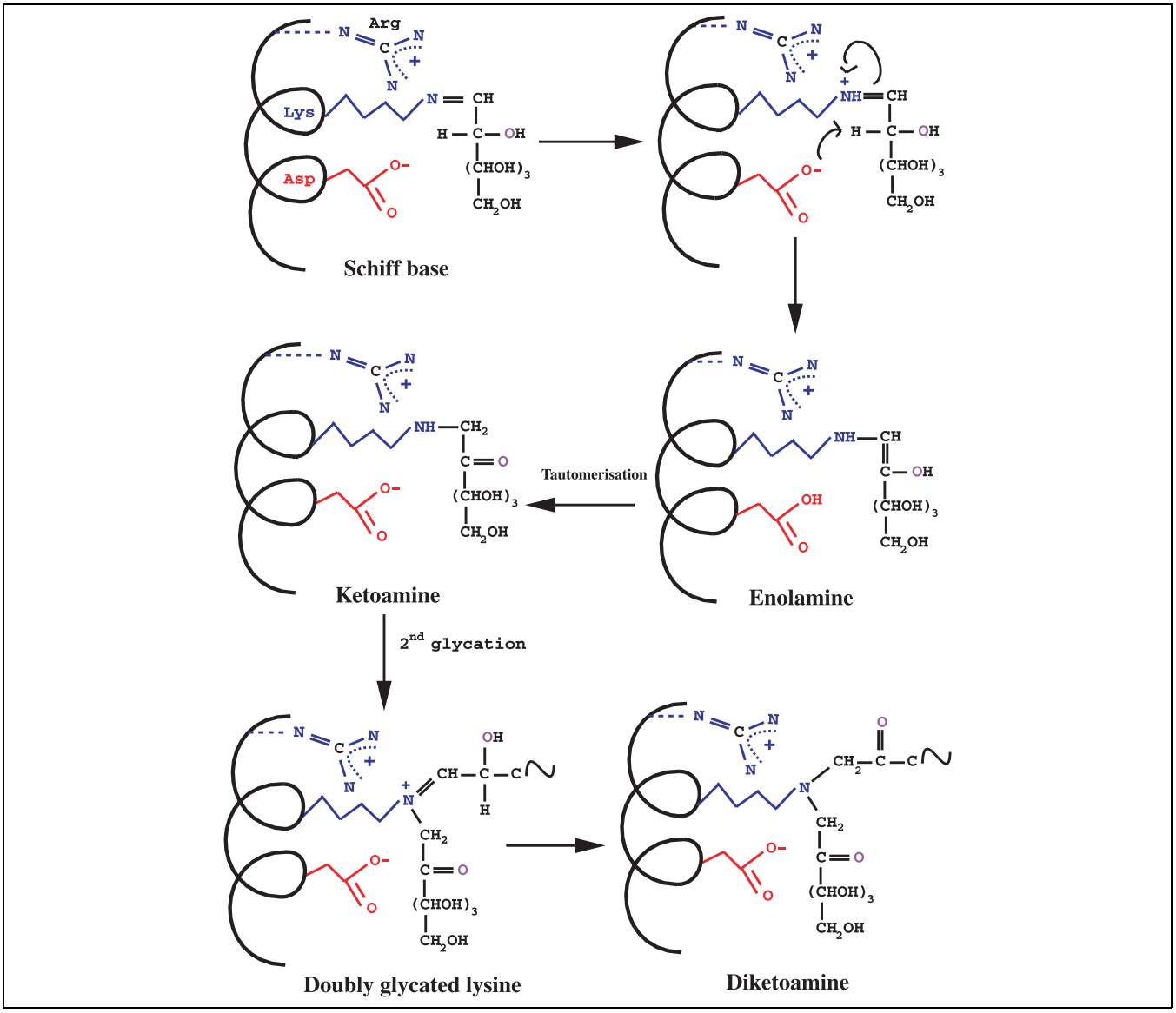

Fig. 11. Schematic representation summarizing the reactions occurring on the model peptide helices and the residues involved. The mechanism of Amadori rearrangement on Lys6 is shown as catalyzed by Asp10. The proximity of the arginine residue and its effect on the reactions involving Lys6 are also highlighted. Peptide RKD4 contains all three residues, while KD4 contains only Lys6 and Asp10.

ilar to KD4 (KD4 caused Amadori rearrangement in ~29% of total glycated peptide at the end of 16 h when RKD4 had catalyzed ketoamine formation in 28% of its glycated component) (Figs. 8a,b and 10). RKD4 also underwent a second glycation reaction (Fig. 8c) with the product bearing two glucose moieties being detected in spectra recorded after 30 h. This bis-glucose adduct, which is a doubly glycated lysine (Fig. 11), also rearranged to form the bis-ketoamine product, as distinguished using hydroxylamine. Subsequently, glycation in terms of both aldimine and ketoamine product formation continued, with the reaction not attaining saturation even after 6 days, when, ~71% of the peptide was glycated, 23% of which was in the doubly glycated form (16.2% of total peptide). ~82% of the glycated component had undergone the Amadori rearrangement.

3. Discussion

Peptide models containing different catalytic residues aid in the study of factors influencing Schiff base formation and Amadori rearrangement in the protein glycation reaction. The use of helical scaffolds permits positioning of catalytic groups proximate to the glycation site. Comparison of the glycation of KD4 with KD2, KH4 and K14 indicates that Schiff base formation in KD4 was the least efficient. The addition of glucose to the ε-amino group of the lysine residue to form a Schiff base is dependent on deprotonation of the charged form of the amino group, which is expected to predominate under the pH conditions used in this study. The spatial proximity of Lys6 and Asp10 in the helical conformation of KD4 might increase the pK_a of the lysine's ε-amino group, hindering deproto-

nation and subsequent glycation. The slower initial glycation rate could affect the overall rate of glycation of KD4, resulting in lower product formation. Conversely, the juxtaposition of Lys6 and Asp10 in KD4 catalyzes the Amadori rearrangement reaction (Fig. 11), resulting in increased amounts of glycated peptide which is resistant to hydrolysis by hydroxylamine. The absence of such an internal catalyst in KD2 results in a slower conversion process despite rapid accumulation of the aldimine product.

Histidine has often been implicated as a catalyst in the glycation reaction because of its unique potential to function as an acid–base catalyst near physiological pH [28,34,35]. Unfortunately, in the in vitro experiments reported here, glycation of the lysine residue is not observed below pH 7.5. Under such conditions of pH, it is likely that only the capacity of histidine to promote proton abstraction in the Amadori rearrangement may be monitored. The diminished Schiff base formation seen in KH4 as compared to K14 (which has no proximate functional residues) seems to suggest that His10 exists in its deprotonated state, and hence perhaps interacts with Lys6. A comparison of peptides KH4 and KD4 suggests that His10 also appears to catalyze the Amadori rearrangement reaction, although less efficiently than aspartic acid.

The positioning of a strongly basic residue such as arginine near Lys6 in peptide RKD4 appears to lower the pK_a of the lysine ε-amino group, resulting in rapid formation of Schiff base adducts. This effect of arginine extends to the glucose–lysine adduct, aiding in the formation of a doubly glycated species (Fig. 11). The double glycation of lysine residues has been previously observed and characterized using ESI-MS-MS in bovine α-crystallin, synthetic peptides derived from the crystallin sequence and *N*-acetyl lysine [66]. In the peptide RKD4, the second glycation on Lys6 has been shown to undergo Amadori rearrangement as well, presumably due to the proximity of the catalytic Asp10. Hence, the ability of the immediate chemical environment to influence both the pK_a of the lysine residue and the conversion of aldimine to ketoamine appears to be important in dictating the course of the glycation reaction at a potential reactive site.

No correlation is observed between the extent of glycation and the helical content of the peptides as detected by CD. Indeed, peptide RKD4, which exhibits the lowest CD ellipticities, appears to glycate most efficiently. Further, peptide KD2, which is similar to RKD4 in its CD characteristics, glycates to a significantly less extent. Thus, secondary structural effects on the glycation reaction appear to be significant only in the context of the local chemical environment provided to the glycation site.

The glycation reactions of all five peptides display a curious dip in glycated peptide amounts after an initial rapid phase of glycation. Examination of the state of glycation at this stage reveals that the glucose–lysine linkage is in the aldimine form (as suggested by the hydroxylamine reaction). The magnitude of the dip varied with the potential of the peptide to catalyze the Amadori rearrangement. The dip is maximum in peptide K14, where the absence of catalytic residues results in virtually no ketoamine product over the time scale investigated. It has been suggested that the aldimine undergoes a competing reaction to release α-oxoaldehydes such as 3-deoxyglucosone, methyl glyoxal and glyoxal [67]. The breakdown of the Schiff base to glyoxal derivatives was proposed by Hayashi and Namiki [68,69]. The observation of maximum loss of glycation in K14, where indeed no subsequent rise in glycation levels was seen, appears to suggest that such an alternative reaction pathway predominates under conditions of poor Amadori conversion of the Schiff base adduct (Fig. 1).

The formation of Schiff base adducts and Amadori products have often been termed the early stages of the glycation reaction. The Amadori product undergoes various oxidation and cross-linking reactions (the late stages of the Maillard reaction) to produce advanced glycation endproducts (AGEs). Many such AGEs have been identified, the most commonly occurring being N^{ε}-carboxymethyl lysine (CML) [70] and pentosidine [71] and their accumulation has been implicated in a variety of age-related disorders [2,9–14,72].

The appearance of a peak in MS experiments corresponding to the mass of CML containing peptide was also observed for peptides KD4, KH4, KD2 and RKD4 at various times. Despite the fact that identical experimental conditions were maintained for all peptides, attempts to rationalize the time of appearance of CML with the catalytic capacity of the peptides was unsuccessful, as CML formation is modulated by a variety of potentially oxidizing conditions [70] which were not controlled in the present studies.

The results described in this report provide a clear demonstration of neighboring group effects in catalyzing glycation at lysine residues in peptides and subsequent irreversible Amadori rearrangement. The study highlights the use of helical scaffolds in dissecting proximity effects in catalysis and emphasizes the utility of ESI-MS as a convenient technique for analyzing glycation reactions.

4. Significance

Both diabetes and ageing are associated with altered glucose metabolism leading to high blood glucose levels, which in turn increase the non-enzymatic glycation of diverse proteins. The reactions characterizing non-enzymatic glycation have been the focus of many studies and the role of neighboring residues or the immediate chemical environment in accelerating these reactions has often been emphasized.

We have attempted to combine the insights obtained from studies on individual proteins in a peptide model, which would provide a single potential glycation site

(a lysine residue) with various chemical environments implicated in the early steps of the glycation reaction. This permits us to independently understand the factors involved in initial Schiff base formation and subsequent Amadori rearrangement in a protein-independent manner. The study clearly demonstrates the role of factors affecting the pK_a of amino groups in stimulating initial glycation and the role of proximate bases in catalyzing the Amadori rearrangement. The additive effects of both features near a potential glycation site, as seen in peptide RKD4, results in accelerated accumulation of irreversibly glycated peptide, which has the capacity to undergo further reactions to form AGEs. The presence of such sites in proteins would greatly aid AGE formation and accumulation, leading to associated disease complications.

Construction of peptide models, which can be easily studied using ESI-MS, permits detailed understanding of the mechanisms underlying such processes, and might also prove to be a convenient platform to test drugs involved in reversing glycation-associated pathology.

5. Materials and methods

5.1. Materials

Chemicals used in solid phase synthetic procedures were obtained from Novabiochem (Nottingham, UK), Bachem (Bubendorf, Switzerland) or Sigma (St. Louis, MO, USA). Trifluoroacetic acid (TFA) and piperidine were purchased from Chem-Impex International Inc. (Wood Dale, IL, USA). The resin (PAL-PEG-PS) used in peptide synthesis was purchased from PerSeptive Biosystems (Hertford, UK). All other chemicals used were from local manufacturers like Ranbaxy and E. Merck India.

5.2. Peptide synthesis

The target peptides were synthesized on a LKB-Biolynx 4175 semi-automatic peptide synthesiser using standard Fmoc (9-fluorenylmethyloxycarbonyl) chemistry and purified by reverse-phase high performance liquid chromatography (HPLC). The peptides were acetylated at the N-terminus prior to cleavage using 1:1 acetic acid/acetic anhydride. The peptides were cleaved as peptide amides from the PAL-resin using 94% (v/v) TFA, 5% (v/v) anisole and 1% (v/v) ethanedithiol. The pure peptides were characterized by ESI-MS and used in all subsequent experiments (Table 1). Concentrations of stock solutions were determined by tyrosine absorbance ($\varepsilon_{275} \sim 1420\ M^{-1}cm^{-1}$)

5.3. Circular dichroism measurements

Circular dichroism spectra were recorded on a JASCO J-715 CD spectropolarimeter. Spectra were recorded between 250 and 195 nm at 0.1 nm intervals with a time constant of 4 s at room temperature. Spectral data were averaged over four separate scans. A rectangular cell of path length 0.1 cm was used for the spectral range with peptide concentration approximately 50 μM. Peptide stock solutions were made in methanol and diluted into methanol or water/methanol mixtures (50% v/v) to the required concentration.

5.4. MS

All electrospray spectra were recorded in the positive ion detection mode on a Hewlett Packard 1100 MSD model electrospray mass spectrometer equipped with a single quadrupole and a conventional electrospray source. Pure water from a Milli Q apparatus (Millipore Inc.) with a conductance of 18.2 mΩ was mixed with equal volume of methanol and used as the running solvent. The solvent flow rate was 30 μl min^{-1}. Approximately 200–300 pmol of sample were injected each time for analysis. The source temperature was kept at 300°C. Ions were extracted with an orifice potential of 4000 V applied at the nebulizer tip. The ionization was pneumatically assisted using a constant flow of pure N_2 gas at 10 l min^{-1} using a Whatman Nitrogen generator. The same gas was used to maintain the nebulizer pressure at 10 bar. The nozzle skimmer potential was kept at 20 V. The mass spectrometer was calibrated using standards supplied by the manufacturer that yield five *m/z* ions across the mass range *m/z* 118–2500. The ion chromatographic peak width for operation was 0.18 min. The cycle time was 1.90 s/cycle and the time filter was kept on. Data were acquired in the scan mode for 2 min and averaged over the complete ion chromatogram to obtain the mass spectrum. The charge states were determined using the isotopic distribution of the peaks and from the difference between the peak values of the protonated species and sodium adducts.

5.5. Reaction of glucose with peptides

Peptide (1 mM in methanol) was mixed with an equal volume of D-glucose (1 M in water) to give a final peptide: glucose ratio of 1:1000 in a 50% (v/v) water/methanol solution. Reaction mixtures were adjusted to a pH of 8.5 using sodium bicarbonate buffer (final concentration 12.5 mM) and incubated at 37°C. Aliquots were removed periodically, diluted 10-fold and analyzed by MS.

5.6. Differentiation between aldimine and ketoamine products

Aliquots of the reaction mixture were periodically diluted 10-fold into a 5 mM solution of hydroxylamine in water (final peptide: hydroxylamine ratio 1:100), incubated for 15 min and analyzed by MS. The commercially available hydrochloride salt of hydroxylamine was neutralized using sodium bicarbonate prior to use (final pH ~ 6.0).

Acknowledgements

We thank P.R. Krishnaswamy, S.G. Vikram and R. Sudha for discussions. K.A. was a summer trainee of the Indian Institute of Science. This investigation was sup-

ported by the Department of Biotechnology as a program grant in the area of Drug and Molecular Design.

References

[1] M. Brownlee, Negative consequences of glycation, Metabolism 49 (Suppl. 1) (2000) 9–13.

[2] D.R. McCance, D.G. Dyer, J.A. Dunn, K.E. Bailie, S.R. Thorpe, J.W. Baynes, T.J. Lyons, Maillard reaction products and their relation to complications in insulin-dependent diabetes mellitus, J. Clin. Invest. 91 (1993) 2470–2478.

[3] S.R. Thorpe, J.W. Baynes, Role of the Maillard reaction in diabetes mellitus and diseases of aging, Drugs Aging 9 (1996) 69–77.

[4] H. Vlassara, M. Brownlee, A. Cerami, Nonenzymatic glycosylation: role in the pathogenesis of diabetic complications, Clin. Chem. 32 (1986) B37–B41.

[5] M. Brownlee, A. Cerami, H. Vlassara, Advanced products of nonenzymatic glycosylation and the pathogenesis of diabetic vascular disease, Diabetes Metab. Rev. 4 (1988) 437–451.

[6] H. Vlassara, H. Fuh, Z. Makita, S. Krungkrai, A. Cerami, R. Bucala, Exogenous advanced glycosylation end products induce complex vascular dysfunction in normal animals: a model for diabetic and aging complications, Proc. Natl. Acad. Sci. USA 89 (1992) 12043–12047.

[7] K.M. Reiser, Nonenzymatic glycation of collagen in aging and diabetes, Proc. Soc. Exp. Biol. Med. 218 (1988) 23–37.

[8] J.L. Wautier, P.J. Guillausseau, Diabetes, advanced glycation endproducts and vascular disease, Vasc. Med. 3 (1998) 131–137.

[9] M.P. Vitek, K. Bhattacharya, J.M. Glendening, E. Stopa, H. Vlassara, R. Bucala, K. Manogue, A. Cerami, Advanced glycation end products contribute to amyloidosis in Alzheimer disease, Proc. Natl. Acad. Sci. USA 91 (1994) 4766–4770.

[10] T.J. Lyons, G. Silvestri, J.A. Dunn, D.G. Dyer, J.W. Baynes, Role of glycation in modification of lens crystallins in diabetic and nondiabetic senile cataracts, Diabetes 40 (1991) 1010–1015.

[11] A. Pande, W.H. Garner, A. Spector, Glucosylation of human lens protein and cataractogenesis, Biochem. Biophys. Res. Commun. 89 (1979) 1260–1266.

[12] M.X. Fu, K.J. Wells-Knecht, J.A. Blackledge, T.J. Lyons, S.R. Thorpe, J.W. Baynes, Glycation, glycoxidation, and cross-linking of collagen by glucose. Kinetics, mechanisms, and inhibition of late stages of the Maillard reaction, Diabetes 43 (1994) 676–683.

[13] M.D. Ledesma, P. Bonay, J. Avila, Tau protein from Alzheimer's disease patients is glycated at its tubulin-binding domain, J. Neurochem. 65 (1995) 1658–1664.

[14] Z. Makita, H. Vlassara, E. Rayfield, K. Cartwright, E. Friedman, R. Rodby, A. Cerami, R. Bucala, Hemoglobin-AGE: a circulating marker of advanced glycosylation, Science 258 (1992) 651–653.

[15] D.W. Allen, W.A. Shroeder, J. Balog, Observations on the chromatographic heterogeneity of normal adult and fetal human hemoglobin: A study of the effects of crystallization and chromatography on the heterogeneity and isoleucine content, J. Am. Chem. Soc. 80 (1958) 1628–1634.

[16] W.R. Holmquist, W.A. Schroeder, A new N-terminal blocking group involving a Schiff base in hemoglobin AIc, Biochemistry 5 (1966) 2489–2503.

[17] R.M. Bookchin, P.M. Gallop, Structure of hemoglobin AIc: nature of the N-terminal beta chain blocking group, Biochem. Biophys. Res. Commun. 32 (1968) 86–93.

[18] H.F. Bunn, D.N. Haney, K.H. Gabbay, P.M. Gallop, Further identification of the nature and linkage of the carbohydrate in hemoglobin A1c, Biochem. Biophys. Res. Commun. 67 (1975) 103–109.

[19] R. Shapiro, M.J. McManus, C. Zalut, H.F. Bunn, Sites of nonenzymatic glycosylation of human hemoglobin A, J. Biol. Chem. 255 (1980) 3120–3127.

[20] A.S. Acharya, L.G. Sussman, J.M. Manning, Schiff base adducts of glyceraldehyde with hemoglobin. Differences in the Amadori rearrangement at the alpha-amino groups, J. Biol. Chem. 258 (1983) 2296–2302.

[21] P. Nacharaju, A.S. Acharya, Amadori rearrangement potential of hemoglobin at its glycation sites is dependent on the three-dimensional structure of protein, Biochemistry 31 (1992) 12673–12679.

[22] R.L. Garlick, J.S. Mazer, The principal site of nonenzymatic glycosylation of human serum albumin in vivo, J. Biol. Chem. 258 (1983) 6142–6146.

[23] N. Iberg, R. Fluckiger, Nonenzymatic glycosylation of albumin in vivo. Identification of multiple glycosylated sites, J. Biol. Chem. 261 (1986) 13542–13545.

[24] E.C. Abraham, M. Cherian, J.B. Smith, Site selectivity in the glycation of alpha A- and alpha B-crystallins by glucose, Biochem. Biophys. Res. Commun. 201 (1994) 1451–1456.

[25] K.M. Reiser, M.A. Amigable, J.A. Last, Nonenzymatic glycation of type I collagen. The effects of aging on preferential glycation sites, J. Biol. Chem. 267 (1992) 24207–24216.

[26] N.G. Watkins, S.R. Thorpe, J.W. Baynes, Glycation of amino groups in protein: Studies on the specificity of modification of RNase by glucose, J. Biol. Chem. 260 (1985) 10629–10636.

[27] R.G. Khalifah, P. Todd, A.A. Booth, S.X. Yang, J.D. Mott, B.G. Hudson, Kinetics of nonenzymatic glycation of ribonuclease A leading to advanced glycation end products. Paradoxical inhibition by ribose leads to facile isolation of protein intermediate for rapid post-Amadori studies, Biochemistry 35 (1996) 4645–4650.

[28] B.H. Shilton, D.J. Walton, Sites of glycation of human and horse liver alcohol dehydrogenase in vivo, J. Biol. Chem. 266 (1991) 5587–5592.

[29] K. Arai, S. Maguchi, S. Fujii, H. Ishibashi, K. Oikawa, N. Taniguchi, Glycation and inactivation of human Cu–Zn-superoxide dismutase. Identification of the in vitro glycated sites, J. Biol. Chem. 262 (1987) 16969–16972.

[30] K.C. Agarwal, R.E. Parks Jr., J.A. Widness, R. Schwartz, Nonenzymatic glycosylation of erythrocytic proteins in normal and diabetic subjects. Enzymes of nucleoside and nucleotide metabolism, Diabetes 34 (1985) 251–255.

[31] T. Kondo, K. Murakami, Y. Ohtsuka, M. Tsuji, S. Gasa, N. Taniguchi, Y. Kawakami, Estimation and characterization of glycosylated carbonic anhydrase I in erythrocytes from patients with diabetes mellitus, Clin. Chim. Acta 166 (1987) 227–236.

[32] S. Ratnaike, D. Blake, P. Shevenan, Enzymic glycation may decrease activity of erythrocytic delta-aminolevulinate dehydratase in diabetes mellitus, Clin. Chem. 33 (1987) 1807–1810.

[33] N.G. Watkins, C.I. Neglia-Fisher, D.G. Dyer, S.R. Thorpe, J.W. Baynes, Effect of phosphate on the kinetics and specificity of glycation of protein, J. Biol. Chem. 263 (1987) 7207–7212.

[34] N. Mori, Y. Bai, H. Ueno, J.M. Manning, Sequence dependent reactivity of model peptides with glyceraldehyde, Carbohydr. Res. 189 (1989) 49–63.

[35] N. Mori, J.M. Manning, Studies on the Amadori rearrangement in a model system: chromatographic isolation of intermediates and product, Anal. Biochem. 152 (1986) 396–401.

[36] I.L. Karle, P. Balaram, Structural characteristics of alpha-helical peptide molecules containing Aib residues, Biochemistry 29 (1990) 6747–6756.

[37] R. Kaul, P. Balaram, Stereochemical control of peptide folding, Bioorg. Med. Chem. 7 (1999) 105–117.

[38] E. Benedetti, X-ray crystallography of peptides: the contributions of the Italian laboratories, Biopolymers 40 (1996) 3–44.

[39] R. Bosch, H. Schmitt, G. Jung, W. Winter, Crystal structure of the α-helical undecapeptide Boc-L-Ala-Aib-Ala-Aib-Ala-Glu(OBzl)-Ala-Aib-Ala-Aib-Ala-OMe, Biopolymers 24 (1985) 961–979.

[40] G.R. Marshall, E.E. Hodgkin, D.A. Langs, G.D. Smith, J. Zabrocki, M.T. Leplawy, Factors governing helical preference of peptides con-

taining multiple alpha, alpha-dialkyl amino acids, Proc. Natl. Acad. Sci. USA 87 (1990) 487–491.

[41] B.V.V. Prasad, P. Balaram, The stereochemistry of peptides containing α-aminoisobutyric acid, CRC Crit. Rev. Biochem. 16 (1984) 307–348.

[42] P. Balaram, De novo design: backbone conformational constraints in nucleating helices and beta-hairpins, J. Pept. Res. 54 (1999) 195–199.

[43] C.A. Rohl, R.L. Baldwin, Deciphering rules of helix stability in peptides, Methods Enzymol. 295 (1998) 1–26.

[44] R.W. Woody, Circular dichroism of peptides, in: S. Udenfriend, J. Meienhofer, V.J. Hruby (Eds.), The Peptides, Conformation in Biology and Drug Design, Academic Press, Orlando, FL, 1985, pp. 15–114.

[45] R.W. Woody, Circular dichroism, Methods Enzymol. 246 (1995) 34–71.

[46] A. Chakrabartty, J.A. Schellman, R.L. Baldwin, Large differences in the helix propensities of alanine and glycine, Nature 351 (1991) 586–588.

[47] A. Chakrabartty, T. Kortemme, S. Padmanabhan, R.L. Baldwin, Aromatic side-chain contribution to far-ultraviolet circular dichroism of helical peptides and its effect on measurement of helix propensities, Biochemistry 32 (1993) 5560–5565.

[48] P. Wallimann, R.J. Kennedy, D.S. Kemp, Large circular dichroism ellipticities for N-templated helical polypeptides are inconsistent with currently accepted helicity algorithms, Angew. Chem. Int. Ed. 38 (1999) 1290–1292.

[49] K.P. Peterson, J.G. Pavlovich, D. Goldstein, R. Little, J. England, C.M. Peterson, What is hemoglobin A1c? An analysis of glycated hemoglobins by electrospray ionization mass spectrometry, Clin. Chem. 44 (1998) 1951–1958.

[50] N.B. Roberts, B.N. Green, M. Morris, Potential of electrospray mass spectrometry for quantifying glycohemoglobin, Clin. Chem. 43 (1997) 771–778.

[51] T. Nakanishi, A. Miyazaki, M. Kishikawa, M. Yasuda, Y. Tokuchi, Y. Kanada, A. Shimizu, Quantification of glycated hemoglobin by electrospray ionization mass spectrometry, J. Mass Spectrom. 32 (1997) 773–778.

[52] M. Saraswathi, T. Nakanishi, A. Shimizu, Relative quantification of glycated Cu–Zn superoxide dismutase in erythrocytes by electrospray ionization mass spectrometry, Biochim. Biophys. Acta 1426 (1999) 483–490.

[53] A. Lapolla, D. Fedele, R. Seraglia, S. Catinella, L. Baldo, R. Aronica, P. Traldi, A new effective method for the evaluation of glycated intact plasma proteins in diabetic subjects, Diabetologia 38 (1995) 1076–1081.

[54] A. Lapolla, D. Fedele, R. Aronica, M. Garbeglio, M. D'Alpaos, R. Seraglia, P. Traldi, The in vivo glyco-oxidation of alpha- and beta-globins investigated by matrix-assisted laser desorption/ionization mass spectrometry, Rapid Commun. Mass Spectrom. 10 (1996) 1133–1135.

[55] A. Lapolla, D. Fedele, R. Aronica, M. Garbeglio, M. D'Alpaos, R. Seraglia, P. Traldi, Evaluation of IgG glycation levels by matrix-assisted laser desorption/ionization mass spectrometry, Rapid Commun. Mass Spectrom. 11 (1997) 1342–1346.

[56] A. Lapolla, D. Fedele, M. Garbeglio, L. Martano, R. Tonani, R. Seraglia, D. Favretto, M.A. Fedrigo, P. Traldi, A highly specific method for the characterization of glycation and glyco-oxidation products of globins, Rapid Commun. Mass Spectrom. 11 (1997) 613–617.

[57] A. Lapolla, D. Fedele, M. Plebani, M. Garbeglio, R. Seraglia, M. D'Alpaos, C.N. Arico, P. Traldi, Direct evaluation of glycated and glyco-oxidized globins by matrix-assisted laser desorption/ionization mass spectrometry, Rapid Commun. Mass Spectrom. 13 (1999) 8–14.

[58] A. Lapolla, D. Fedele, M. Garbeglio, L. Martano, R. Tonani, R. Seraglia, D. Favretto, M.A. Fedrigo, P. Traldi, Matrix-assisted laser desorption/ionization mass spectrometry, enzymatic digestion, and molecular modeling in the study of nonenzymatic glycation of IgG, J. Am. Soc. Mass Spectrom. 11 (2000) 153–159.

[59] H. Odani, Y. Matsumoto, T. Shinzato, J. Usami, K. Maeda, Mass spectrometric study on the protein chemical modification of uremic patients in advanced Maillard reaction, J. Chromatogr. B Biomed. Sci. Appl. 731 (1999) 131–140.

[60] R.H. Zaugg, J.A. Walder, I.M. Klotz, Schiff base adducts of hemoglobin. Modifications that inhibit erythrocyte sickling, J. Biol. Chem. 252 (1977) 8542–8548.

[61] H.S. Isbell, H.L. Frush, Mutarotation, hydrolysis and rearrangement reactions of glycosylamines, J. Org. Chem. 23 (1958) 1309–1319.

[62] E.H. Cordes, W.P. Jencks, Semicarbazone formation from pyridoxal, pyridoxal phosphate and their Schiff bases, Biochemistry 1 (1962) 773–778.

[63] E.H. Cordes, W.P. Jencks, Nucleophilic catalysis of semicarbazone formation by anilines, J. Am. Chem. Soc. 84 (1962) 826–831.

[64] H. Wada, E.E. Snell, The enzymatic oxidation of pyridoxine and pyridoxamine phosphates, J. Biol. Chem. 236 (1961) 2089–2095.

[65] A.S. Acharya, J.M. Manning, Amadori rearrangement of glyceraldehyde-hemoglobin Schiff base adducts. A new procedure for the determination of ketoamine adducts in proteins, J. Biol. Chem. 255 (1980) 7218–7224.

[66] R. Blakytny, J.A. Carver, J.J. Harding, G.W. Kilby, M.M. Sheil, A spectroscopic study of glycated bovine alpha-crystallin: investigation of flexibility of the C-terminal extension, chaperone activity and evidence for diglycation, Biochim. Biophys. Acta 1343 (1997) 299–315.

[67] P.J. Thornalley, A. Langborg, H.S. Minhas, Formation of glyoxal, methylglyoxal and 3-deoxyglucosone in the glycation of proteins by glucose, Biochem. J. 344 (1999) 109–116.

[68] T. Hayashi, M. Namiki, Formation of two-carbon sugar fragment at an early stage of the browning reaction of sugar wth amine, Agric. Biol. Chem. 44 (1980) 2575–2580.

[69] T. Hayashi, M. Namiki, Role of sugar fragmentation in the Maillard reaction, Dev. Food Sci. 13 (1986) 29–38.

[70] M.U. Ahmed, S.R. Thorpe, J.W. Baynes, Identification of N epsilon-carboxymethyllysine as a degradation product of fructoselysine in glycated protein, J. Biol. Chem. 261 (1986) 4889–4894.

[71] D.R. Sell, V.M. Monnier, Structure elucidation of a senescence cross-link from human extracellular matrix. Implication of pentoses in the aging process, J. Biol. Chem. 264 (1989) 21597–21602.

[72] K.J. Wells-Knecht, E. Brinkmann, M.C. Wells-Knecht, J.E. Litchfield, M.U. Ahmed, S. Reddy, D.V. Zyzak, S.R. Thorpe, J.W. Baynes, New biomarkers of Maillard reaction damage to proteins, Nephrol. Dial. Transplant. 11 (1996) 41–47.